JOURNAL OF GUIDANCE, CONTROL, AND DYNAMICS
Vol. 41, No. 12, December 2018

Engineering Notes

Nonlinear Analytical Equations of Relative Motion on J_2-Perturbed Eccentric Orbits

Bradley Kuiack* and Steve Ulrich†
Carleton University, Ottawa, Ontario K1S 5B6, Canada

DOI: 10.2514/1.G003723

I. Introduction

SPACECRAFT formation flying is rapidly becoming a key space technology, which increases the performance, the cost-effectiveness, and the flexibility of an operational mission. Examples of spacecraft formation-flying missions include GRACE [1], TanDEM-X [2], and PRISMA [3]. Despite the success of these missions, future formation-flying missions will have to satisfy increasingly challenging functional and performance requirements in their guidance, navigation, and control (GN&C) tasks. In particular, guidance and control algorithms and their implementation must comply with limited on-board processing resources and propellant. The guidance system is responsible for calculating the desired relative motion trajectory to be tracked by the control system during reconfiguration maneuvers between the initial (current) and the desired (future) formation defined by the user. In this paper, a simple, yet accurate and fuel-efficient, guidance law for spacecraft formation flying is sought. More specifically, this paper proposes a guidance law based on nonlinear analytical equations of motion for J_2-perturbed, eccentric orbits. Furthermore, a guidance law is developed in such a way that it lends itself easily to a proven impulsive control method—specifically the impulsive controller from Schaub and Alfriend [4].

Although there are analytical solutions for the exact nonlinear differential equations of relative motion in the local-vertical-local-horizontal (LVLH) reference frame, these solutions have their limitations as a result of imposing certain restrictions in their derivations. The Hill–Clohessy–Wiltshire (HCW) model [5] is one such example where the derived time-explicit closed-form analytical solution is only valid for circular Keplerian orbits. Work by Sabol and McLaughlin [6] used this model to demonstrate that the in-plane and out-of-plane nondrifting relative motion about a circular Keplerian orbit always follows an ellipse centered on the reference orbit. To overcome the inherent limitations of the HCW model, some formulations also take into account orbit perturbations, such as the J_2 perturbation. The J_2 perturbation is particularly important in formation flying because its secular effects on an orbit, that is, the rotation of the line of apsides and precession of the line of nodes, cause secular drift between two J_2-perturbed spacecraft. The introduction of J_2 in a linearized set of equations, similar to the HCW equations, has been proposed by Schweighart and Sedwick [7]. Specifically, the authors developed a set of linear, constant-coefficient, second-order differential equations of motion by considering the orbit-averaged impact of J_2 on a circular reference orbit. An analytical solution to these differential equations was also presented.

However, assuming a circular reference orbit yields considerable errors when the eccentricity of the reference orbit increases. In fact, it has been shown that the errors introduced in the HCW equations by considering an elliptical reference orbit dominate the errors due to ignoring J_2 [8]. For this reason, several formulations have been proposed to model the relative motion about unperturbed elliptical orbits [9–11]. In particular, the linear-time-invariant (LTI) HCW equations have been extended to arbitrary eccentricity by Inalhan et al. [8] by formulating the dynamics as a linear-parameter-varying (LPV) system. Such a dynamics model is especially well suited for controller design purposes, by making use of LPV control techniques, such as model predictive control [12]. Making use of the fact that the orbit angular rate and the radius are functions of the true anomaly, these equations can also be expressed using true anomaly derivatives instead of time derivatives [13]. The resulting differential equations are also time-varying, but are not parameter-varying because the true anomaly has been used to formulate the derivatives. Solutions to these linear-time-varying (LTV) equations are available in the literature in various forms using different reference frames and variables. The first derivation with singularities in the closed-form solution was provided by Lawden [14]. Then, Carter [15] provided a set of solutions without singularities. These homogenous solutions are extremely useful for well-behaved numerical and analytical analysis on the shape, structure, and optimization of passive apertures in eccentric reference orbits. Interestingly, the same solutions can be obtained via incremental changes in orbital elements, as demonstrated by Marec [16]. Lane and Axelrad [17] developed a time-explicit closed-form solution and studied the relative motion for bounded elliptical orbits. Melton [18] also proposed an alternative solution for small eccentricity reference orbits. Recent work from Guffanti et al. [19] approaches the problem of analytical propagation of satellite relative motion in perturbed, eccentric orbits using a relative orbital element state representation augmented with force model parameters. The resulting formulations capture the secular and long-periodic effects of the perturbations, but average out the short-periodic effects. Recent work from Mahajan, Vadali, and Alfriend has presented a sophisticated model for analytically propagating relative motion with second-order short-periodic and secular effects, and first-order long-periodic effects for arbitrary zonal harmonics [20]. The same authors have also worked on propagating spacecraft motion on arbitrary eccentricity orbits while taking into account tesseral and sectorial spherical harmonics via the Delaunay normalization of the perturbed Keplerian Hamiltonian [21].

A closed-form analytical solution that is valid for Keplerian eccentric orbits was developed by Gurfil and Kholshevnikov [22,23]. This simple analytical solution explicitly parameterizes the relative motion using classical orbital elements as constants of the unperturbed Keplerian orbit, instead of Cartesian initial conditions. This concept, originally suggested by Hill [24], has been widely used in the analysis of relative spacecraft dynamics [25,26].

In view of the above, the main contribution of this paper consists in the development of nonlinear, analytical equation of relative motion that are applicable to J_2-perturbed eccentric orbits. To do so, the results of Gurfil and Kholshevnikov [22,23] are herein extended by using J_2-perturbed osculating orbital elements in the solution instead of constant orbital elements. Specifically, J_2-perturbed osculating orbital elements are obtained by adding mean orbital elements to the J_2-induced short-periodic variations. The accuracy of this new analytical solution will then validated through comparison with a numerical simulator, and is compared with the accuracy of the

Received 5 April 2018; revision received 5 June 2018; accepted for publication 6 June 2018; published online 12 October 2018.

*Graduate Student, Department of Mechanical and Aerospace Engineering, 1125 Colonel By Drive.

†Associate Professor, Department of Mechanical and Aerospace Engineering, 1125 Colonel By Drive. Senior Member AIAA.

original Gurfil and Kholshevnikov solution. Finally, this paper develops a terminal-point guidance law based on the back-propagation of these equations. The resulting guidance law is then validated in a closed-loop guidance control scenario, demonstrating its efficiency in terms of propellant consumption for a reconfiguration maneuver.

Although simpler than more sophisticated methods being developed for propagating perturbed relative motion analytically, this paper may provide a slightly different viewpoint on developing relative motion methodologies. Specifically, the methodology presented here lends itself to a relative motion viewpoint involving relative distances, or metrics, as the work is a direct continuation of the method presented by Gurfil and Kholshevnikov in their work on metrics [23]. Thus, a contribution of this Note is to demonstrate the effectiveness of the newly proposed analytical equations of relative motion, and to demonstrate their use in a closed-loop-control scenario.

The remainder of this paper is organized as follows: Sec. II reviews the original solution to the relative motion on eccentric orbits problem proposed by Gurfil and Kholshevnikov [22,23], Sec. III presents the newly developed analytical solution for relative motion on J_2-perturbed eccentric orbits, Sec. IV compares the accuracy of the new solution with a numerical simulator, Sec. V presents the use of the new equations in a terminal-point guidance system and demonstrates the use of this guidance in a closed-loop control simulation, and finally Sec. VI provides concluding remarks.

II. Gurfil and Kholshevnikov Solution

As previously mentioned, works by Gurfil and Kholshevnikov [22,23] form the basis for the analytical solution derived herein. In their work, the authors proposed a simple method of calculating the relative position of a follower spacecraft with respect to a leader using orbital elements. This allows the equations of relative motion to remain accurate for arbitrarily large values of eccentricity. To do so, consecutive rotations and a translation are applied to obtain an analytical expression for $\boldsymbol{\rho}$, which denotes the components of the relative position vector in the LVLH reference frame, denoted $\mathcal{F}_L$, that is

$$\boldsymbol{\rho} = \boldsymbol{r}_L - \boldsymbol{r}'_L \tag{1}$$

where $\boldsymbol{r}_L$ and $\boldsymbol{r}'_L$, respectively, denote the components of the follower and leader spacecraft position vector expressed in $\mathcal{F}_L$. In Eq. (1), the term $\boldsymbol{r}_L$ is obtained from $\boldsymbol{r}_P$, that is, its components in its perifocal frame, $\mathcal{F}_P$, using three subsequent rotations in a 3-1-3 sequence as follows:

$$\boldsymbol{\rho} = \boldsymbol{C}_{LP'}(\nu')\, \boldsymbol{C}_{P'I}(\omega', i', \Omega')\boldsymbol{C}_{\text{IP}}(\omega, i, \Omega)\boldsymbol{r}_P - \boldsymbol{r}'_{L'} \tag{2}$$

where i, ω, and Ω, respectively, denote the inclination, argument of perigee, and right ascension of the ascending node of the spacecraft, and the superscript $\{\}'$ symbol refers to the leader spacecraft of the formation, with the lack of this superscript indicating the follower. The rotation matrices used in Eq. (2) are defined as follows:

$$\boldsymbol{C}_{\text{IP}}(\omega, i, \Omega) = \begin{bmatrix} c_\Omega c_\omega - s_\Omega s_\omega c_i & -c_\Omega s_\omega - s_\Omega c_\omega c_i & s_\Omega s_i \\ s_\Omega c_\omega + c_\Omega s_\omega c_i & -s_\Omega s_\omega - c_\Omega c_\omega c_i & -c_\Omega s_i \\ s_\omega s_i & c_\omega s_i & c_i \end{bmatrix} \tag{3}$$

$$\boldsymbol{C}_{P'I}(\omega', i', \Omega') = \begin{bmatrix} c_{\Omega'} c_{\omega'} - s_{\Omega'} s_{\omega'} c_{i'} & s_{\Omega'} c_{\omega'} + c_{\Omega'} s_{\omega'} c_{i'} & s_{\omega'} s_{i'} \\ -c_{\Omega'} s_{\omega'} - s_{\Omega'} c_{\omega'} c_{i'} & -s_{\Omega'} s_{\omega'} - c_{\Omega'} c_{\omega'} c_{i'} & c_{\omega'} s_{i'} \\ s_{\Omega'} s_{i'} & -c_{\Omega'} s_{i'} & c_{i'} \end{bmatrix} \tag{4}$$

$$\boldsymbol{C}_{LP'}(\nu') = \begin{bmatrix} c_{\nu'} & s_{\nu'} & 0 \\ -s_{\nu'} & c_{\nu'} & 0 \\ 0 & 0 & 1 \end{bmatrix} \tag{5}$$

where the notations c_x and s_x represent the cosine and sine function of the variable x, respectively, used here to keep the rotation matrices to a manageable size. $\boldsymbol{r}_P$ and $\boldsymbol{r}'_L$ are given by

$$\boldsymbol{r}_P = [\, r\cos\nu \quad r\sin\nu \quad 0\,]^T \tag{6}$$

$$\boldsymbol{r}'_L = [\, r' \quad 0 \quad 0\,]^T \tag{7}$$

where ν denotes the true anomaly and r denotes the orbit radius obtained from the orbit equation as follows:

$$r = \frac{a(1-e^2)}{1 + e\cos\nu} \tag{8}$$

where a denotes the semimajor axis, and e denotes the eccentricity of the orbit. The orbit radius of the leader can be determined by using the leader's orbital elements in Eq. (8). Note that Eq. (2) can be written component-wise and further simplified through the use of relative orbital elements. For more details, the readers are referred to Refs. [22,23].

III. Analytical Relative Motion Solution on J_2-Perturbed Eccentric Orbits

For ease of use as a guidance law, the relative motion solution should be described in a set of three analytical equations; one for each direction of the local-vertical-local-horizontal reference frame $\mathcal{F}_L$. From Eq. (2), the following set of three equations can be obtained:

$$\begin{aligned} x(t) &= r\cos\nu(k'_1 k_1 + k'_2 k_4 + k'_3 k_7) + r\sin\nu(k'_1 k_2 + k'_2 k_5 + k'_3 k_8) - r' \\ y(t) &= r\cos\nu(k'_4 k_1 + k'_5 k_4 + k'_6 k_7) + r\sin\nu(k'_4 k_2 + k'_5 k_5 + k'_6 k_8) \\ z(t) &= r\cos\nu(k'_7 k_1 + k'_8 k_4 + k'_9 k_7) + r\sin\nu(k'_7 k_2 + k'_8 k_5 + k'_9 k_8) \end{aligned} \tag{9}$$

where the constants, denoted by k's, are herein defined as

$$\begin{aligned} k_1 &= \cos\Omega\cos\omega - \sin\Omega\sin\omega\cos i \\ k_2 &= -\cos\Omega\sin\omega - \sin\Omega\cos\omega\cos i \\ k_3 &= \sin\Omega\sin i \\ k_4 &= \sin\Omega\cos\omega + \cos\Omega\sin\omega\cos i \\ k_5 &= -\sin\Omega\sin\omega - \cos\Omega\cos\omega\cos i \\ k_6 &= -\cos\Omega\sin i \\ k_7 &= \sin\omega\sin i \\ k_8 &= \cos\omega\cos i \\ k_9 &= \cos i \end{aligned} \tag{10}$$

$$\begin{aligned} k'_1 &= \cos\Omega'\cos u' - \sin\Omega'\sin u'\cos i' \\ k'_2 &= \sin\Omega'\cos u' + \cos\Omega'\sin u'\cos i' \\ k'_3 &= \sin u'\sin i' \\ k'_4 &= -\cos\Omega'\sin u' - \sin\Omega'\cos u'\cos i' \\ k'_5 &= -\sin\Omega'\sin u' - \cos\Omega'\cos u'\cos i' \\ k'_6 &= \cos u'\sin i' \\ k'_7 &= \sin\Omega'\sin i' \\ k'_8 &= -\cos\Omega'\sin i' \\ k'_9 &= \cos i' \end{aligned} \tag{11}$$

Note that u is the argument of latitude, defined as the sum of ν and ω, which allows the matrices from Eqs. (4) and (5) to be combined as follows:

$$\boldsymbol{C}_{L'I}(u', i', \Omega') = \begin{bmatrix} c_{\Omega'} c_{u'} - s_{\Omega'} s_{u'} c_{i'} & s_{\Omega'} c_{u'} + c_{\Omega'} s_{u'} c_{i'} & s_{u'} s_{i'} \\ -c_{\Omega'} s_{u'} - s_{\Omega'} c_{u'} c_{i'} & -s_{\Omega'} s_{u'} - c_{\Omega'} c_{u'} c_{i'} & c_{u'} s_{i'} \\ s_{\Omega'} s_{i'} & -c_{\Omega'} s_{i'} & c_{i'} \end{bmatrix} \tag{12}$$

Equation (9), along with definitions of constants previously defined, is simply a more compact way of expressing the Gurfil and Kholshevnikov solution presented in the previous section. This is an exact solution for the relative position of a follower spacecraft in $\mathcal{F}_L$ as long as the orbital elements used in the calculation of this relative position are accurate. Assuming that the orbital elements are constant leads to an exact solution for relative position on Keplerian orbits. The same equations can be applied with the J_2-perturbed osculating orbital elements to obtain a relative position solution that accounts for the J_2 perturbation.

It should be noted that using Eq. (9) in this way implies that the expressions in Eqs. (10) and (11) are not truly constants, but functions of time (this is not shown in the equations). This means that they must be calculated at a given time to find the relative position, but they still serve to help simplify the equations of relative position. The use of J_2-perturbed osculating orbital elements implies that the orbital elements used to calculate each constant in Eqs. (10) and (11) are also functions of time, but the (t) notation is omitted here to aid in the readability of the expressions.

The J_2-perturbed osculating orbital elements can be approximated by adding the mean orbital elements to the time-varying short-periodic variation of each element caused by J_2, as follows:

$$\begin{aligned} a &= \bar{a} + \Delta a_{\text{sp}} \\ e &= \bar{e} + \Delta e_{\text{sp}} \\ i &= \bar{i} + \Delta i_{\text{sp}} \\ \omega &= \bar{\omega} + \Delta \omega_{\text{sp}} \\ \Omega &= \bar{\Omega} + \Delta \Omega_{\text{sp}} \\ M &= \bar{M} + \Delta M_{\text{sp}} \end{aligned} \tag{13}$$

where $\bar{\{\}}$ denotes the mean orbital element and $\Delta\{\}_{\text{sp}}$ denotes the short-periodic variation of the element as a result of the J_2 perturbation. In Eq. (13) the mean anomaly, denoted as M, is used in place of true anomaly, but the values are closely related, and the true anomaly can be found easily from the mean anomaly as will be shown later in the paper. These expressions for the J_2-perturbed osculating orbital elements are not exact as there are higher-order effects on the orbital elements caused by J_2. For example, there are also long-periodic variations. However, using the sum of the mean orbital elements and these short-periodic variations is a reasonably accurate method of accounting for the J_2-perturbation in the short-term, thereby balancing accuracy and complexity.

The mean semimajor axis, eccentricity, and inclination have no secular variation caused by J_2, and are therefore equal to their initial mean values, that is, $\bar{a} = \bar{a}_0$, $\bar{e} = \bar{e}_0$, and $\bar{i} = \bar{i}_0$, as well as $\bar{a}' = \bar{a}'_0$, $\bar{e}' = \bar{e}'_0$, and $\bar{i}' = \bar{i}'$. The mean orbital motion and mean semilatus rectum for each spacecraft, $\{\bar{n}, \bar{p}\}$ and $\{\bar{n}', \bar{p}'\}$ for the follower and leader spacecraft, respectively, are only functions of mean semimajor axis and mean eccentricity, that is,

$$\bar{n} = \sqrt{\frac{\mu}{\bar{a}^3}} \tag{14}$$

$$\bar{p} = \bar{a}(1 - \bar{e}^2) \tag{15}$$

The remaining mean orbital elements, $\{\bar{\omega}, \bar{\Omega}, \bar{M}\}$ and $\{\bar{\omega}', \bar{\Omega}', \bar{M}'\}$, can be propagated forward in time, from t_0 to t, by summing initial mean orbital elements with the J_2-induced secular variations, as follows:

$$\begin{aligned} \bar{\omega} &= \bar{\omega}_0 + \dot{\bar{\omega}} t \\ \bar{\Omega} &= \bar{\Omega}_0 + \dot{\bar{\Omega}} t \\ \bar{M} &= \bar{M}_0 + \dot{\bar{M}} t \end{aligned} \tag{16}$$

where the secular variations due to J_2 are given by [27]

$$\dot{\bar{\omega}} = \frac{1}{2}\bar{n}J_2\left(\frac{R_e}{\bar{p}}\right)^2(4 - 5\sin^2\bar{i}) \tag{17}$$

$$\dot{\bar{\Omega}} = -\frac{3}{2}\bar{n}J_2\left(\frac{R_e}{\bar{p}}\right)^2\cos\bar{i} \tag{18}$$

$$\dot{\bar{M}} = \bar{n} + \frac{3}{2}\bar{n}J_2\left(\frac{R_e}{\bar{a}}\right)^2\frac{1}{(1-\bar{e}^2)^{3/2}}\left(1 - \frac{3}{2}\sin^2\bar{i}\right) \tag{19}$$

The short-periodic variations for each spacecraft are calculated as a function of the osculating orbital elements, as follows [28]:

$$\begin{aligned} \Delta a_{\text{sp}} = \frac{J_2R_e^2}{a}\Bigg[&\left(\frac{a}{r}\right)^3 - \frac{1}{(1-e^2)^{3/2}} + \left\{-\left(\frac{a}{r}\right)^3 + \frac{1}{(1-e^2)^{3/2}}\right. \\ &\left. + \left(\frac{a}{r}\right)^3\cos(2\omega + 2\nu)\right\}\frac{3\sin^2 i}{2}\Bigg] \end{aligned} \tag{20}$$

$$\begin{aligned} \Delta e_{\text{sp}} = \frac{J_2R_e^2}{4}\Bigg[&\frac{-2}{a^2e\sqrt{1-e^2}} + \frac{2a(1-e^2)}{er^3} + \left\{\frac{3}{a^2e\sqrt{1-e^2}}\right. \\ &- \frac{3a(1-e^2)}{er^3} - \frac{3(1-e^2)\cos(\nu + 2\omega)}{p^2} - \frac{3\cos(2\nu + 2\omega)}{a^2e(1-e^2)} \\ &\left. + \frac{3a(1-e^2)\cos(2\nu + 2\omega)}{er^3} - \frac{(1-e^2)\cos(3\nu + 2\omega)}{p^2}\right\}\sin^2 i\Bigg] \end{aligned} \tag{21}$$

$$\begin{aligned} \Delta i_{\text{sp}} = \frac{J_2R_e^2\sin(2i)}{8p^2}&[3\cos(2\omega + 2\nu) + 3e\cos(2\omega + \nu) \\ &+ e\cos(2\omega + 3\nu)] \end{aligned} \tag{22}$$

$$\begin{aligned} \Delta\Omega_{\text{sp}} = \frac{J_2R_e^2\cos(i)}{4p^2}&[6(\nu - M + e\sin\nu) - 3\sin(2\omega + 2\nu) \\ &- 3e\sin(2\omega + \nu) - e\sin(2\omega + 3\nu)] \end{aligned} \tag{23}$$

$$\begin{aligned} \Delta\omega_{\text{sp}} = \frac{3J_2R_e^2}{2p^2}\Bigg[&\left(2 - \frac{5}{2}\sin^2 i\right)(\nu - M + e\sin\nu) \\ &+ \left(1 - \frac{3}{2}\sin^2 i\right)\left\{\frac{1}{e}\left(1 - \frac{1}{4}e^2\right)\sin\nu + \frac{1}{2}\sin(2\nu) + \frac{e}{12}\sin(3\nu)\right\} \\ &- \frac{1}{e}\left\{\frac{1}{4}\sin^2 i + \left(\frac{1}{2} - \frac{15}{16}\sin^2 i\right)e^2\right\}\sin(\nu + 2\omega) + \frac{e}{16}\sin^2 i\sin(\nu - 2\omega) \\ &- \frac{1}{2}\left(1 - \frac{5}{2}\sin^2 i\right)\sin(2\nu + 2\omega) + \frac{1}{e}\left\{\frac{7}{12}\sin^2 i - \frac{1}{6}\left(1 - \frac{19}{8}\sin^2 i\right)e^2\right\} \\ &\times\sin(3\nu + 2\omega) + \frac{3}{8}\sin^2 i\sin(4\nu + 2\omega) + \frac{e}{16}\sin^2 i\sin(5\nu + 2\omega)\Bigg] \end{aligned} \tag{24}$$

$$\begin{aligned} \Delta M_{\text{sp}} = \frac{3J_2R_e^2\sqrt{1-e^2}}{2ep^2}\Bigg[&-\left(1 - \frac{3}{2}\sin^2(i)\right)\left\{\left(1 - \frac{e^2}{4}\right)\sin\nu \right. \\ &\left. + \frac{e}{2}\sin(2\nu) + \frac{e^2}{12}\sin(3\nu)\right\} + \sin^2 i\left\{\frac{1}{4}\left(1 + \frac{5}{4}e^2\right)\sin(\nu + 2\omega)\right. \\ &- \frac{e^2}{16}\sin(\nu - 2\omega) - \frac{7}{12}\left(1 - \frac{e^2}{28}\right)\sin(3\nu + 2\omega) \\ &\left. - \frac{3e}{8}\sin(4\nu + 2\omega) - \frac{e^2}{16}\sin(5\nu + 2\omega)\right\}\Bigg] \end{aligned} \tag{25}$$

where the true anomaly can be calculated from the mean anomaly as follows:

$$\nu = \tan^{-1} \frac{\sqrt{1-e^2}\sin E}{\cos E - e} \tag{26}$$

where

$$E = M + e\sin(M + e\sin(M + e\sin(M+, \cdots, +e\sin(M)))) \tag{27}$$

with the number of terms used in the approximation in Eq. (27) can be adjusted to increase accuracy. Using these above expressions, accurate approximations for the J_2-perturbed orbital elements for both a leader and follower spacecraft in formation are obtained analytically, and used with Eq. (9) to find the relative position between both spacecraft.

IV. Numerical Simulations

To verify the accuracy of the newly developed method of calculating the relative position between two spacecraft, numerical simulations are performed in MATLAB. The results obtained with the analytical solution provided in this paper were compared with a simulator that numerically integrates the exact, nonlinear differential equations of motion in $\mathcal{F}_I$. Specifically, the simulator integrates, for each spacecraft, the inertial two-body equations of motion to which the J_2 inertial perturbing acceleration is added. Both spacecraft position vectors are then transformed into $\mathcal{F}_L$. Finally, the leader position vector is subtracted from the follower position vector, to obtain $\boldsymbol{\rho}$. The simulator was initialized using, for both spacecraft, the initial osculating orbital elements that were converted into components of the initial position and velocity vectors in $\mathcal{F}_I$. The exact same initial osculating orbital elements were also used to initialize the proposed method of calculating relative position outlined in the previous section. Unless otherwise specified in the

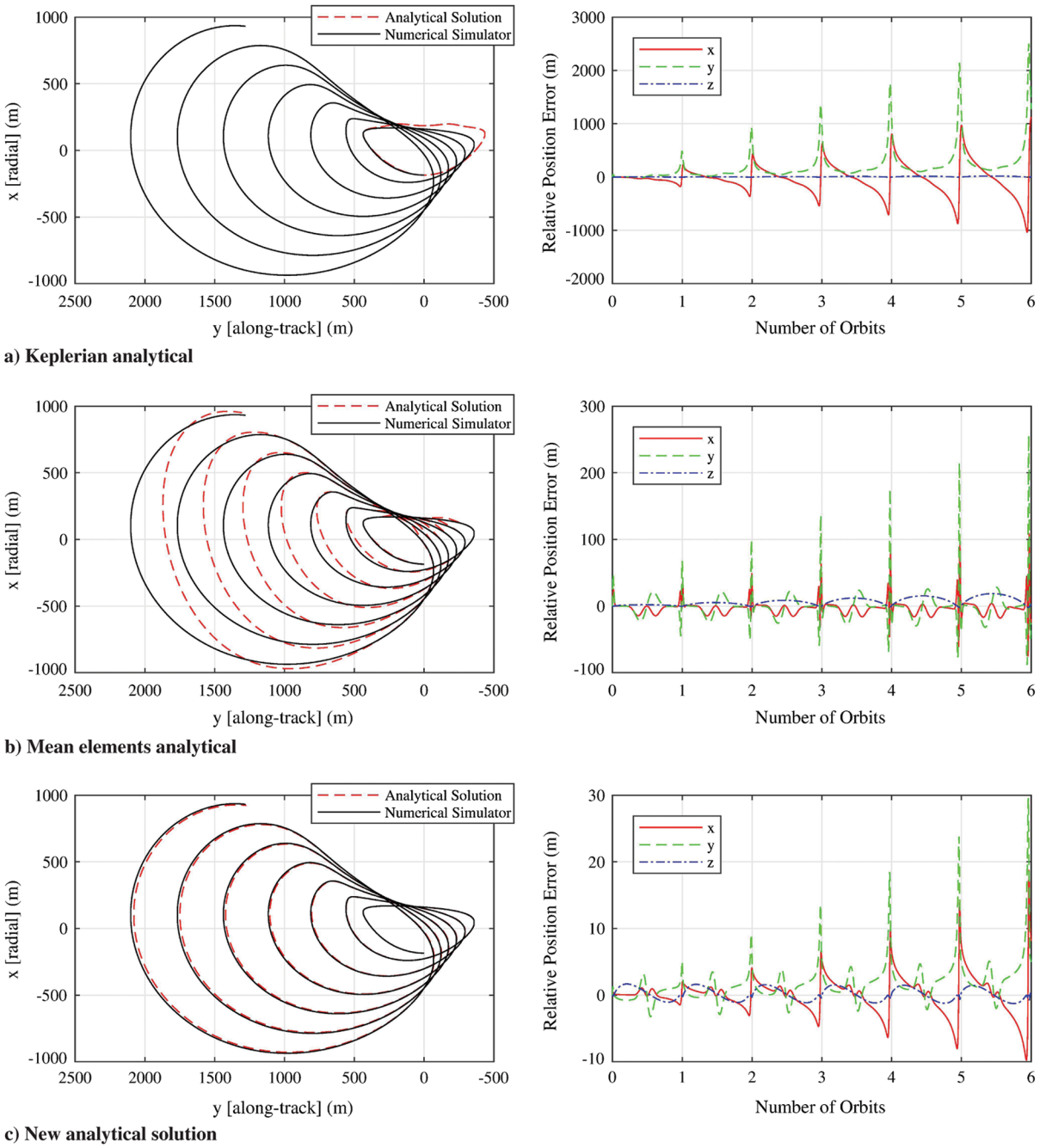

a) Keplerian analytical

b) Mean elements analytical

c) New analytical solution

Fig. 1 Analytical solutions compared with numerical simulator for PROBA-3 example.

Table 1 Initial osculating orbital elements

Orbital element	Leader	Follower
Semimajor axis, km	7106.14	a'
Eccentricity	0.05	$e' + 0.001$
Inclination, deg	98.3	98.3
Argument of perigee, deg	0	0
Right ascension of the ascending node, deg	270	270
True anomaly, deg	0	0

captions of the subsequent figures (or in the text in the case of Fig. 1), Table 1 presents the initial osculating orbital elements used for both models (numerical simulator and analytical equations). The orbital elements given in this table correspond to a simple in-plane elliptical formation.

Each of the figures in this section presents three analytical solutions for comparison with the numerical simulator. First, the numerical simulator was compared with the original Gurfil and Kholshevnikov equations without any modification, and therefore with no attempt to account for the J_2 perturbation. Second, the numerical simulator is compared with the Gurfil and Kholshevnikov solution using the initial mean orbital elements in the analytical solution instead of initial osculating orbital elements. This is accomplished by rearranging Eq. (13) to solve for the mean orbital elements, or in other words by subtracting by the initial short periodic variations caused by J_2 [from Eqs. (20–25)] from the initial osculating orbital elements. This represents a case in between simply using the original Gurfil and Kholshevnikov equations and propagating the J_2-perturbed osculating orbital elements. It still accounts for the J_2 perturbation to some extent, namely, by evaluating the effect of J_2 on the initial orbital elements, but does not

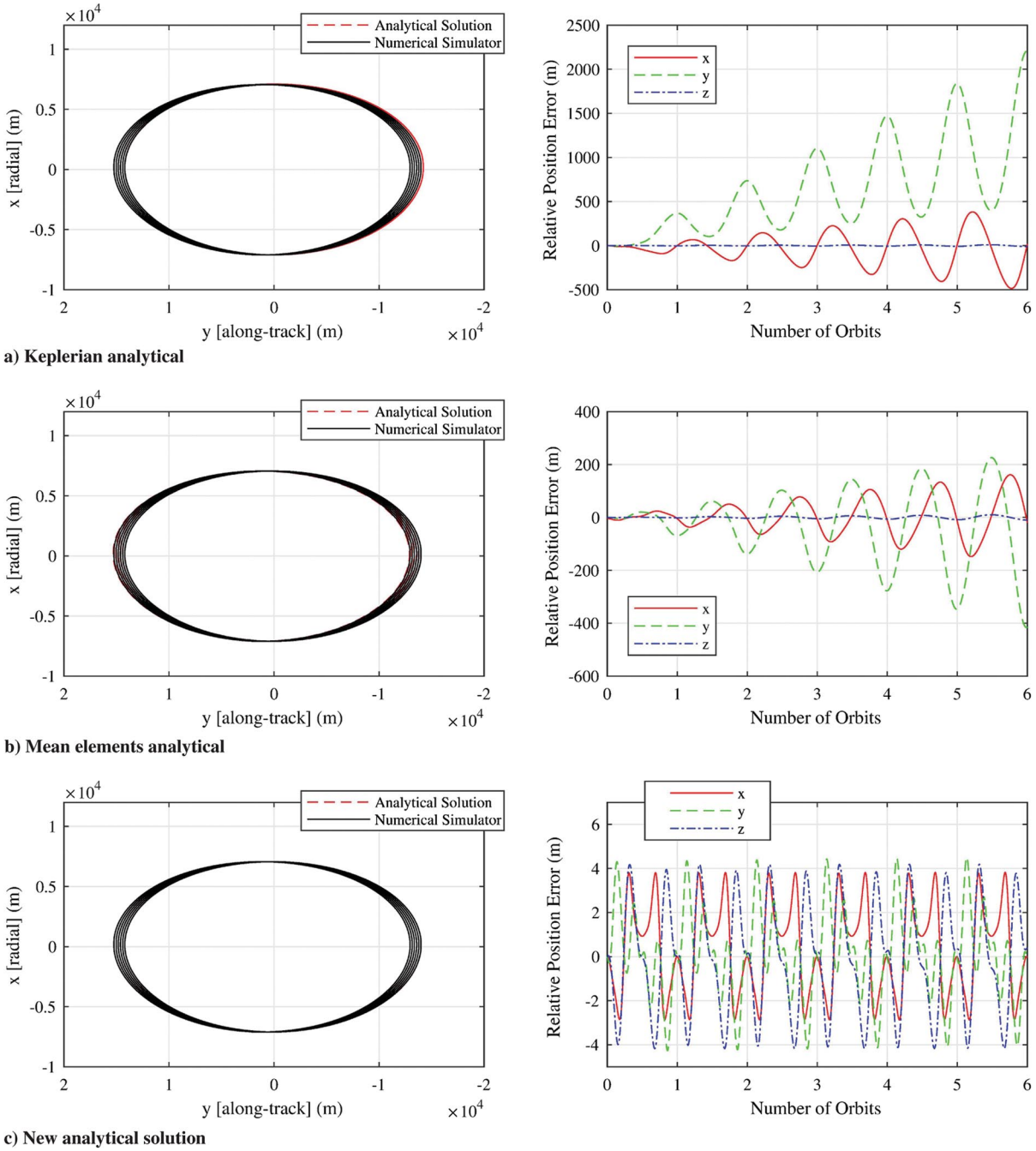

Fig. 2 Analytical solutions compared with numerical simulator.

continue to follow the osculating orbital elements. It is therefore much less computational intensive than the new solution proposed in this paper, but still offers improvement over the original Gurfil and Kholshevnikov solution. Finally, the numerical simulator is also compared with the new equations derived in the previous section. The in-plane motion (on the left side of the figures) and the position error (on the right side of the figure), defined as the difference between the analytical solution and the numerical simulator are given for each of the three cases, labeled a), b), and c), respectively.

Figure 2 reports the results obtained by propagating the relative motion at a relatively low eccentricity over six orbits with the analytical equations and the numerical simulator. The use of the new equations greatly reduces error compared with the Gurfil and Kholshevnikov solution when the orbit is J_2-perturbed. This error remains bounded (for all practical purposes) with an accuracy better than 5 m along each direction. Although there is a slight increase in the error in the along-track direction, this minimal drift is negligible over the six orbital periods shown. It is interesting to note that the error when using initial mean orbital elements is significantly improved compared with using initial osculating orbital elements. In other words, a more accurate solution can be obtained from the Gurfil and Kholshevnikov solution by converting the initial conditions to mean orbital elements, which requires little computational effort. Then, if an even more accurate solution is desired, the new equations accounting for the short-periodic variations throughout the orbits can be used at the expense of a heavier computational load.

Another interesting note that should be made is that the error differences between using initial mean and initial osculating orbital elements is greatest if the initial conditions are near perigee. The reason for this is that the short-periodic variations affecting most of the orbital elements tend to reach their highest magnitudes near these points. Intuitively, at orbit points where the short-periodic variations

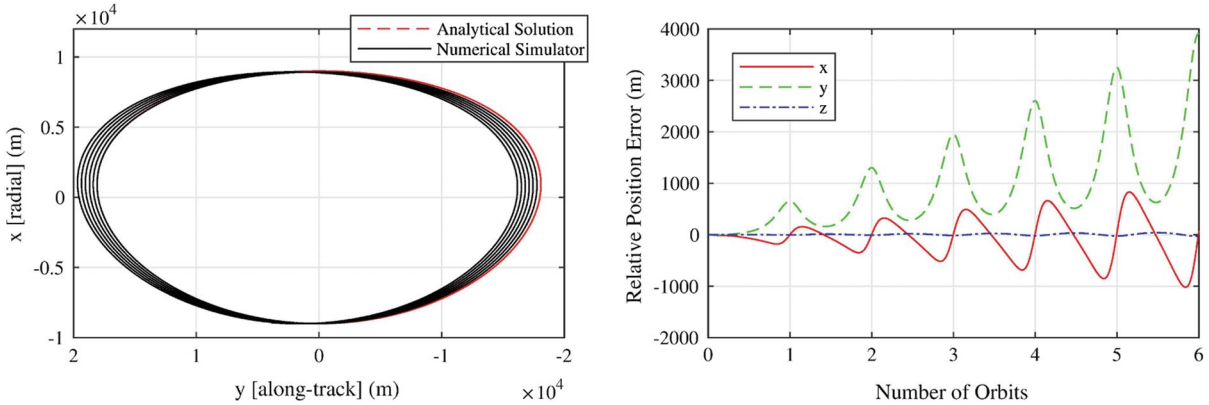

a) Keplerian analytical

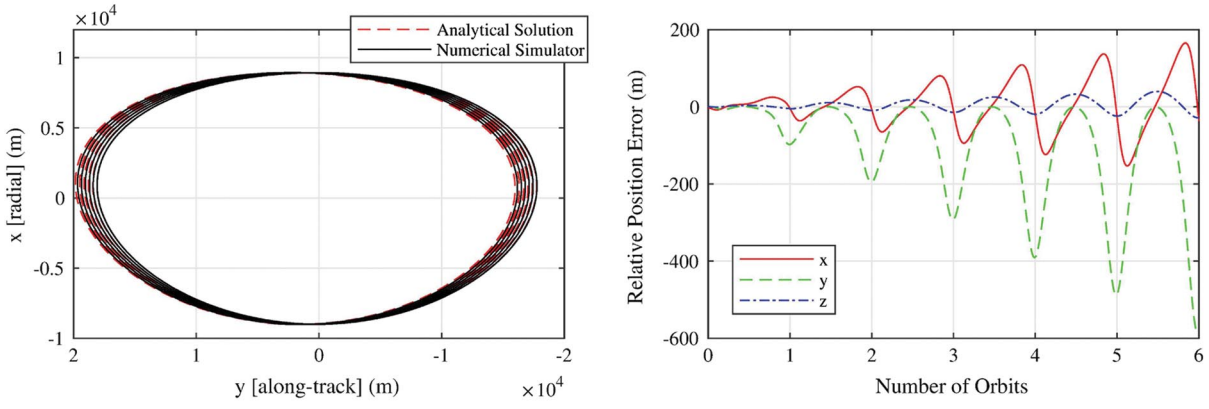

b) Mean elements analytical

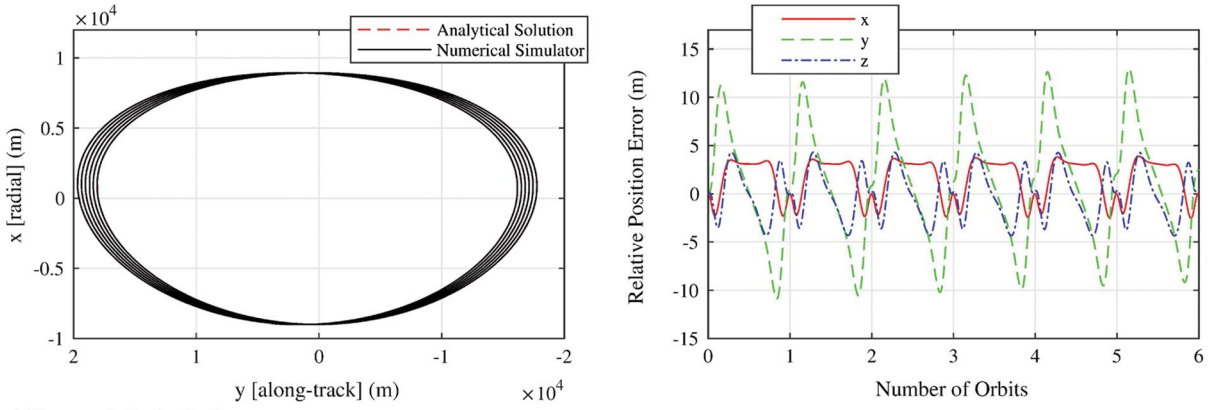

c) New analytical solution

Fig. 3 Analytical solutions compared with numerical simulator for $e' = 0.2$ and $a' = 9\,000$ km.

are smallest, the difference between mean and J_2-perturbed osculating orbital elements is small, and the errors resulting from initializing the Gurfil and Kholshevnikov solution with either of them become similar.

Figure 3 shows the results obtained when the leader reference orbit is significantly more elliptical. As before, the accuracy of the analytical solutions increases from a) to c) as would be expected for taking into account the J_2 perturbation to greater degrees. Similarly to the previous near-circular orbit case, the errors are practically bounded for the new equations, and the new analytical solution is representative of the actual spacecraft motion, as predicted by the numerical simulator. However, it is clear that as the eccentricity increases, the ability of the analytical solution to track the relative motion accurately decreases. This is especially true in the along-track direction, where the error increases significantly with increase in eccentricity.

To further study the application of the proposed analytical solution for formations on a highly-eccentric orbit (HEO), the relative equations of motion were applied to case similar to the European Space Agency's PROBA-3 mission. This Sun observation mission will involve two spacecraft in precise formation in highly eccentric orbits, with the formation forming a solar coronagraph. The PROBA-3 leader's orbit is defined with $a'_0 = 37040$ km, $e'_0 = 0.806$, $i'_0 = 59$ deg, $\Omega'_0 = 84$ deg, and $\omega'_0 = 188$ deg, as well as a spacecraft separation on the order of 100 m [29]. Setting up a simulation with two spacecraft in this orbit, with the follower eccentricity given by $e = e' + 0.000005$ is a gross simplification of the ultimate relative motion for the mission, but it may still provide

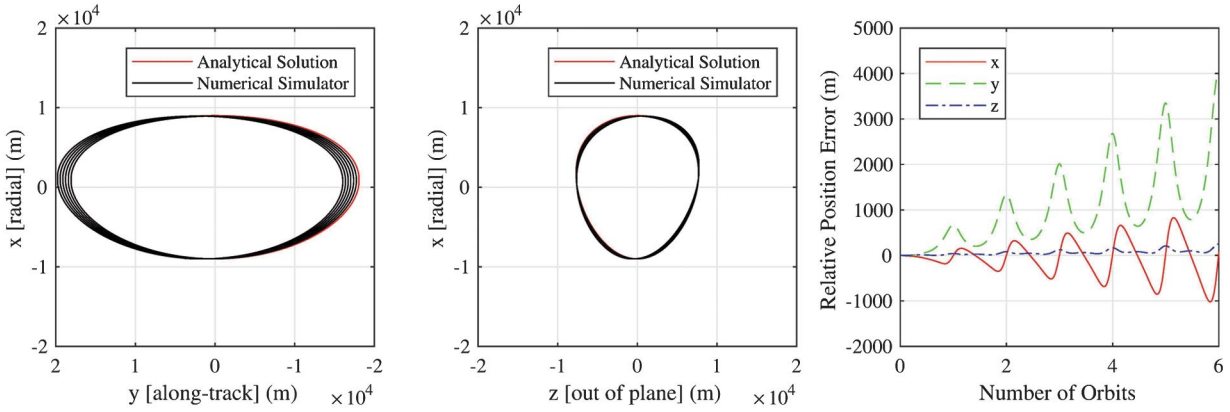

a) Keplerian analytical

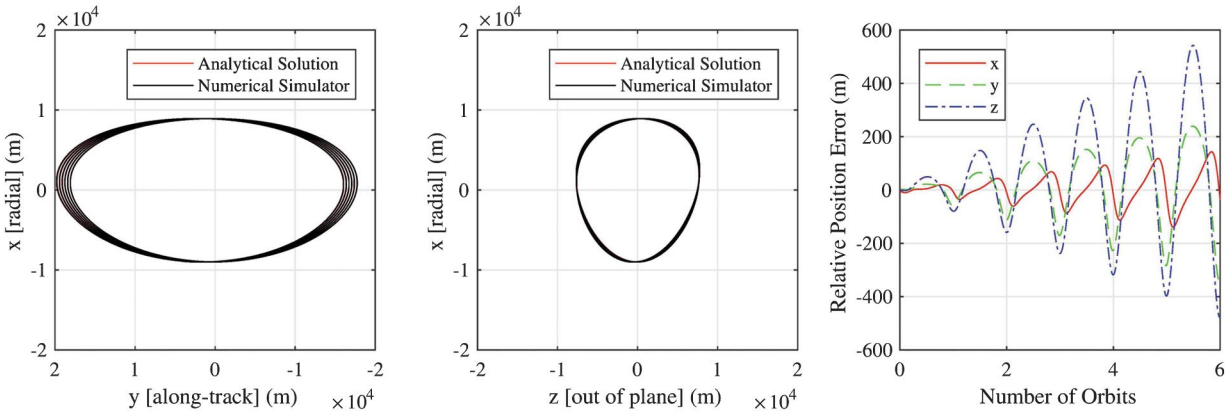

b) Mean elements analytical

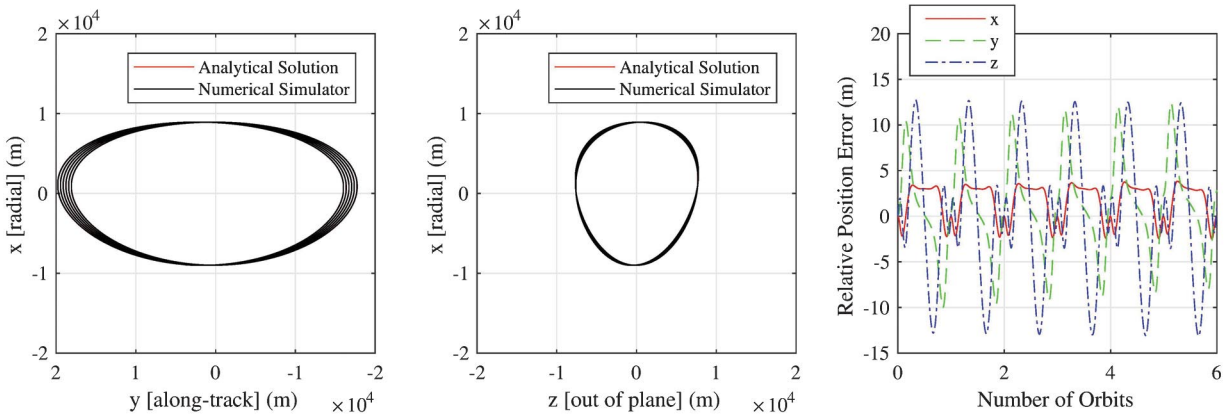

c) New analytical solution

Fig. 4 Analytical solutions compared with numerical simulator for $e' = 0.2$ and $a' = 9000$ km and $i = i' + 0.05$ deg.

some insight regarding the accuracy of the proposed analytical solution in a HEO. Figure 1 shows the results of the simulation. Although the resulting errors are unbounded for the new equations, the error is controlled quite well, staying below 30 m over six orbital periods.

In each of the previous cases, the formation was defined such that there is no out-of-plane motion. To assess the ability of the analytical solution to handle out-of-plane motion, another simulation was performed with a small inclination difference between the two spacecraft. The result is reported in Fig. 4. This figure shows that the equations can indeed handle out-of-plane motion.

Each of Figs. 2–4 illustrates the improvement of the new equations over the original Gurfil and Kholshevnikov equations, and also proves the good accuracy obtained from using the new analytical solution.

V. Back-Propagation Guidance Law for Reconfiguration Maneuvers

Another benefit to the new analytical equations of relative motion is that they can easily be propagated both backward and forward in time. This has potential applications in spacecraft formation flying, as often times the desired final configuration of the formation is known, but at the present the spacecraft may be in some arbitrary configuration. By taking the desired spacecraft dynamics at some known time in the future, and back-propagating through the previously presented equations of relative motion, the ideal motion of each spacecraft at the present time can be calculated. That is, the position and velocity of each spacecraft at the present time that will passively result in the desired formation at the future time can be calculated. In many situations this should result in fuel savings, as instead of letting the spacecraft track some arbitrary relative motion until a specific relative motion is required and then performing the required Δv maneuvers, the spacecraft are initially placed (using smaller Δv maneuvers) onto a trajectory that naturally drifts, thanks to J_2, toward the desired final formation.

A. Back-Propagating the Nonlinear Analytical Equations of Motion

Back-propagation can be implemented through the nonlinear J_2-perturbed analytical equations of relative motion in a similar way to what is commonly done for the HCW linear equations of motion. Instead of starting a scenario with initial conditions, the scenario is started with desired final conditions for each spacecraft, in the form of final osculating orbital elements. These elements are then propagated backward from zero to the negative of the final time, while taking into account the J_2 perturbation. Finally, along the way, the relative position of the two spacecraft can be solved for based on the time-varying orbital elements.

A simulation was performed to validate the accuracy of the back-propagation guidance strategy. A desired final relative position of spacecraft was defined, and then propagated backward to the initial time. The relative position at the initial time was then propagated forward in time with a numerical simulator. Figure 5 compares the time-history of the relative position components in $\mathcal{F}_\mathcal{L}$ obtained from the back-propagation guidance strategy against those obtained from the numerical simulator.

Looking at Fig. 5, it can be seen that, although there are small differences between the relative positions obtained from back-propagation and the numerical simulation, the back-propagation models accurately the relative motion. These results prove that the concept of back-propagation guidance can be used with the newly developed equations to accurately determine the necessary initial conditions of spacecraft in formation to passively achieve some desired final relative position in the future.

B. Closed-Loop Implementation

One potential application of the back-propagation guidance strategy is to use it to perform more efficient reconfiguration maneuvers. The idea is that, instead of performing maneuvers at the time that the spacecraft are required to be in a specific configuration, more efficient maneuvers can be performed at some earlier time, placing the spacecraft in a position that will allow them to drift naturally into the desired final configuration.

To test the feasibility of this concept, let us assume an active follower spacecraft to be maneuvered closer to an uncontrolled leader spacecraft. The orbital elements of the leader are known, as is a desired set of orbital elements for the follower spacecraft corresponding to a simple in-plane elliptical formation, which should be achieved within 10 orbital periods of the leader. The orbital elements for the initial position of the follower are also known.

Two cases can be compared in this scenario, with both accomplishing the desired reconfiguration maneuvers after 10 orbital periods. In the first case, a maneuver is performed to achieve the desired final formation immediately before the formation is required, based on the motion of each spacecraft at that time. In the second case, a more efficient strategy is implemented, which corresponds to the newly developed back-propagation guidance law that finds the set of orbital elements at the initial time that will lead to the desired final orbital elements at the final time. A maneuver is then applied immediately to achieve this *ideal* set of initial orbital elements, and

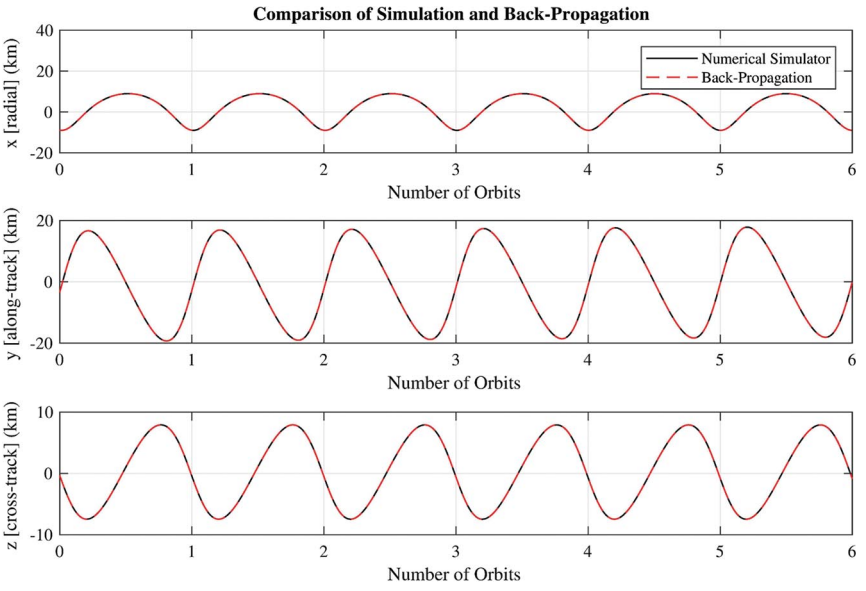

Fig. 5 Comparison of relative position from numerical simulator and back-propagation.

Table 2 Orbital elements for closed-loop guidance and control simulation

Orbital element	Desired leader final	Desired follower final	Follower initial
Semimajor axis, km	15,000	15,000	15,010
Eccentricity	0.2	0.201	0.21
Inclination, deg	59	59	58
Argument of perigee, deg	20	20	20.3
RAAN, deg	84	84	83.5
True anomaly, deg	3	3	2

Table 3 Comparison of required Δv for the two simulation cases

Maneuver	Case 1	Case 2
Δv_h, m/s	140.6	149.7
$\Delta v_{r_p,1}$, m/s	0	0
$\Delta v_{r_a,1}$, m/s	0	0
$\Delta v_{t_p,1}$, m/s	10.1	10.2
$\Delta v_{t_a,1}$, m/s	13.5	13.5
$\Delta v_{r_p,2}$, m/s	42.0	11.4
$\Delta v_{r_a,2}$, m/s	41.4	10.2
$\Delta v_{t_p,2}$, m/s	1.2	1.3
$\Delta v_{t_a,2}$, m/s	0.2	0.2
Total Δv, m/s	249.0	196.5

the spacecraft is allowed to drift naturally into the desired configuration, thereby minimizing fuel consumption.

C. Control Method Selection

To assess the potential benefits of the proposed back-propagation method in a closed-loop scenario, the back-propagation guidance law is combined with the impulsive feedback control method proposed by Schaub and Alfriend [4]. This particular control scheme is convenient, as the impulsive maneuvers are quite simple to implement, and the Δv maneuvers are defined in terms of orbital element differences. For completeness, this impulsive control law is summarized in this subsection.

This control method consists of five different impulsive maneuvers that are applied at three different locations over the course of an orbit. The first maneuver corrects the inclination and the right ascension of the ascending node of the spacecraft, and is fired in the orbit normal direction; the magnitude of the impulse is given by

$$\Delta v_h = (h/r)\sqrt{\delta i^2 + \delta\Omega^2 \sin i^2} \tag{28}$$

where h is orbital angular momentum, r is the spacecraft position magnitude, and δi and $\delta\Omega$ are the orbital element differences, defined as the desired final orbital element subtracted by the current orbital element. This maneuver must take place at a critical true latitude angle defined (between 0 and 180 deg) as

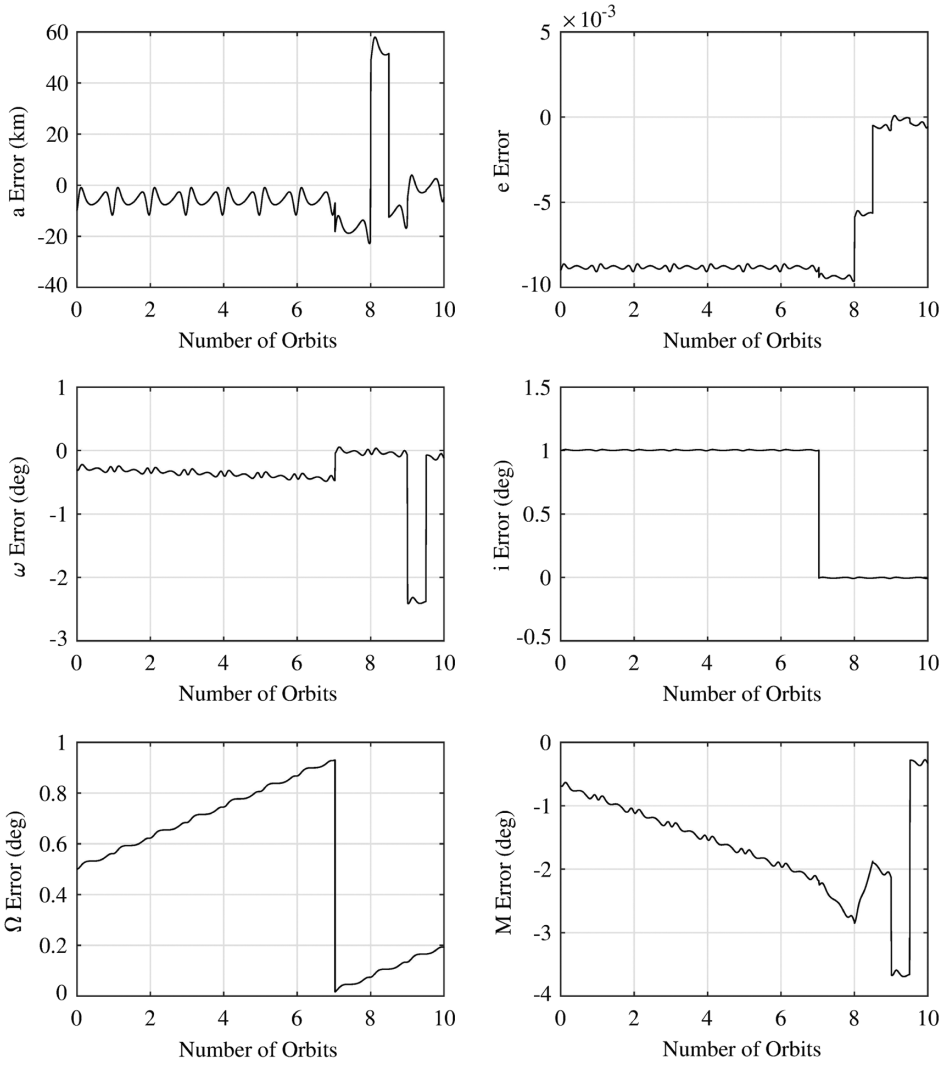

Fig. 6 Closed-loop back-propagation guidance and impulsive control performance validation for case 1.

$$u_c = \tan^{-1}(\delta\Omega \sin i/\delta i) \tag{29}$$

This first maneuver is only meant to affect the inclination and right ascension of the ascending node; however, it should be noted that it will also affect the argument of perigee. This effect will be accounted for in the equations for the next maneuvers, which correct the argument of perigee and mean anomaly errors. To correct these two elements, two maneuvers are performed, one at perigee and one at apogee, each in the radial direction. The two maneuvers are defined in the following equations:

$$\Delta v_{r_p} = -(na/4)\{[(1+e)^2/n](\delta\omega + \delta\Omega\cos i) + \delta M\} \tag{30}$$

$$\Delta v_{r_a} = (na/4)\{[(1-e)^2/n](\delta\omega + \delta\Omega\cos i) + \delta M\} \tag{31}$$

The final two maneuvers are performed to correct the semimajor axis and the eccentricity error, with one taking place at perigee and one at apogee. In this case, each maneuver is fired in the tangential direction, and the magnitude of the respective impulsive maneuvers is defined as

$$\Delta v_{t_p} = (na\eta/4)[\delta a/a + \delta e/(1+e)] \tag{32}$$

$$\Delta v_{t_a} = (na\eta/4)[\delta a/a - \delta e/(1-e)] \tag{33}$$

where $\eta = \sqrt{1-e^2}$.

By performing these five maneuvers over the course of an orbit, the desired set of orbital elements for a spacecraft can be achieved. It should be noted that the two apogee and two perigee maneuvers can be performed simultaneously, and thus the five maneuvers are performed at three discrete points in the orbit.

D. Simulation Results

To verify the practical application of the new equations of relative motion, along with the proposed idea of back-propagation, a simulation was performed. The simulation follows the scenario outlined previously in this section. The orbital elements for the leader and follower spacecraft are given in Table 2.

In this scenario, the desired final configuration must be achieved 10 orbital periods from the initial time, and only the follower is controlled. As previously discussed, there exists two potential methods of achieving the final configuration, both using the same impulsive control method. In case 1, the follower is uncontrolled until closer to the final time, at which point, based on the current orbital elements, the impulsive control law is applied. In case 2, back-propagation is used to determine a set of *ideal* orbital elements at the initial time, the impulsive control law is immediately applied, and the spacecraft drift into the desired formation for the rest of the simulation time. Although in each case a similar maneuver is used, the magnitude of impulsive control inputs applied in each case will vary as a result of the orbital elements varying with time due to J_2. In other words, the objective of case 2 and the back-propagation method is to take advantage of the effects of the J_2 perturbation.

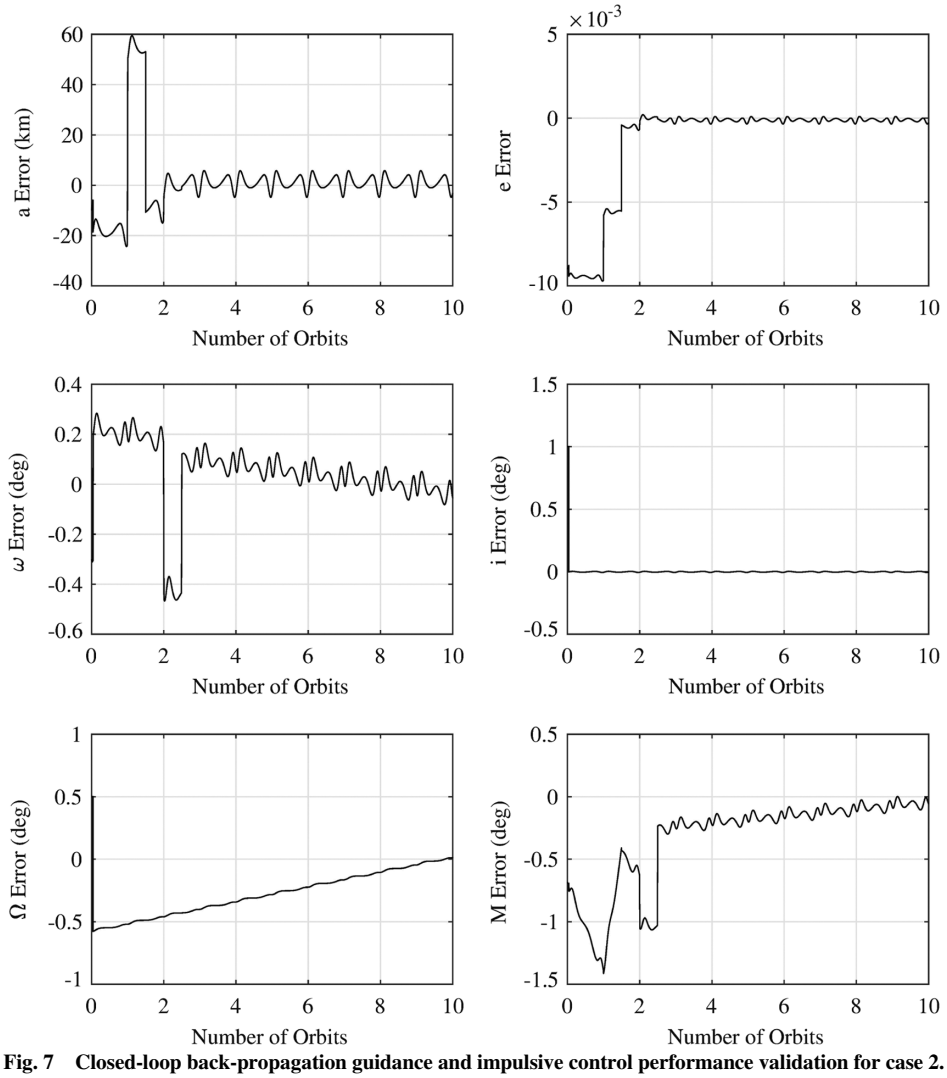

Fig. 7 Closed-loop back-propagation guidance and impulsive control performance validation for case 2.

It should also be noted here that, in an effort to correct the orbital elements better, two sets of tangential in-plane maneuvers were applied. The magnitudes of the second set of maneuvers were calculated based on the orbital element errors after the first set of maneuvers was applied. Only one set of radial maneuvers is applied, and these maneuvers take place with the second tangential maneuvers, when the semimajor axis and eccentricity have already been corrected to be closer to the desired values. The magnitudes of the impulsive maneuvers are summarized in Table 3. Additionally, to validate that the spacecraft was being controlled correctly, the orbital element errors (defined as the desired orbital elements subtracted by the actual orbital elements) for cases 1 and 2 for the follower spacecraft are provided in Figs. 6 and 7.

As shown in Figs. 6 and 7, the control maneuvers successfully correct the orbital elements. There are still errors in each orbital element after 10 orbits, but these errors are small compared with the initial errors. In a real-world scenario it would be more realistic to perform multiple sets of maneuvers (more than two) over the course of a few orbits to ensure that the orbital elements are corrected perfectly. It also should be noted that, as can be seen in Figs. 6 and 7, each orbital element does vary somewhat with time due to J_2, affecting the orbital elements through periodic variations.

Table 3 shows that case 2 uses significantly less Δv to accomplish the same reconfiguration maneuver. From this table, it is clear that, although there might be small differences between the Δv for each maneuver, case 2's decreased fuel usage is mainly a result of much smaller radial Δv maneuvers. This is expected, as the Δv differences are a function of the effects of the J_2 perturbation on the orbital elements. For most of the orbital elements, J_2 has very little effect over the course of 10 orbits, or no effect at all. However, the difference between desired and actual mean anomaly does vary significantly over the course of a few orbits, due both to a difference in period of the spacecraft, and a relative drift between the spacecraft due to J_2. The mean anomaly difference (δM) directly affects the radial Δv maneuvers.

It should be noted that in this particular scenario the back-propagation method is more efficient mainly because, based on the initial conditions, the spacecraft would tend to drift apart from each other. In cases where the spacecraft would initially drift closer to their desired formation, the improvement from using the back-propagation guidance will almost certainly be much less, and in some cases the better option may actually be to perform the maneuvers later in time without using this guidance strategy. Ideally, spacecraft in formation would be able to plan multiple potential maneuvers based on their predicted motion, and choose the most efficient option.

Overall, the numerical simulation results successfully demonstrate that the back-propagation method for performing reconfiguration maneuvers of spacecraft in formation can be successfully integrated with an impulsive controller for reconfiguration purposes. Additionally, the simulation demonstrates a potential application of the back-propagation guidance method and the new equations of relative motion, validating that these new methods can be used to plan more efficient maneuvers.

VI. Conclusions

A set of nonlinear analytical equations for the relative motion between two spacecraft in formation that is applicable to a wide variety of orbits, and also takes into account the J_2 perturbation was derived in this Note. These equations take into account the J_2 perturbation through the use of time-varying expressions that simplify the rotation of vectors between reference frames. One benefit of the new equations is the ease with which they can be used to predict relative motion through forward and backward propagation. Specifically, the concept of back-propagation is introduced as a method of determining efficient reconfiguration maneuvers based on a desired set of final relative orbital elements, thereby allowing the formation to naturally drift into the desired configuration. This concept was tested in a closed-loop control scenario using an impulsive controller demonstrating that maneuvers based on back-propagation can effectively reconfigure the formation, and, in many cases, will be more fuel-efficient than other maneuvers resulting in the same desired relative motion. Future work will focus on implementing the new guidance and control methods in a more realistic hardware-in-the-loop situation, implementing other control methods with the new guidance equations, and the use of more sophisticated guidance systems with the analytical equations. Of particular interest is the possibility of using an impulsive controller that takes into account the J_2 perturbation to further reduce propellant usage, and the possibility of a guidance system that searches for the optimal time for performing back-propagation maneuvers.

Acknowledgments

This work was financially supported by the Natural Sciences and Engineering Research Council of Canada through the Canada Graduate Scholarship CGS M-472002-2017. The authors would also like to thank all of the reviewers for their thoughtful feedback, which helped to strengthen this Note.

References

[1] Presti, D., Herman, J., and Codazzi, A., "Mission Operations System Design and Adaptations for the Twin-Satellite Mission GRACE," *SpaceOps Conference*, Montreal, 2004. doi:10.2514/6.2004-382-219

[2] Kahle, R., Schlepp, B., Aida, S., Kirschner, M., and Wermuth, M., "Flight Dynamics Operations of the TanDEM-X Formation," *SpaceOps Conference*, Stockholm, 2012. doi:10.2514/6.2012-1275094

[3] D'Amico, S., Ardaens, J.-S., and Larsson, R., "Spaceborne Autonomous Formation-Flying Experiment on the PRISMA Mission," *Journal of Guidance, Control, and Dynamics*, Vol. 35, No. 3, 2012, pp. 834–850. doi:10.2514/1.55638

[4] Schaub, H., and Alfriend, K. T., "Impulsive Feedback Control to Establish Specific Mean Orbit Elements of Spacecraft Formations," *Journal of Guidance, Control, and Dynamics*, Vol. 24, No. 4, 2001, pp. 739–745. doi:10.2514/2.4774

[5] Clohessy, W. H., and Wiltshire, R. S., "Terminal Guidance System for Satellite Rendezvous," *Journal of the Aerospace Sciences*, Vol. 27, No. 9, 1960, pp. 653–658. doi:10.2514/8.8704

[6] Sabol, C., and McLaughlin, C. A., "Satellite Formation Flying Design and Evolution," *Journal of Spacecraft and Rockets*, Vol. 38, No. 2, 2001, pp. 270–278. doi:10.2514/2.3681

[7] Schweighart, S. A., and Sedwick, R. J., "High-Fidelity Linearized J_2 Model for Satellite Formation Flight," *Journal of Guidance, Control, and Dynamics*, Vol. 25, No. 6, 2002, pp. 1073–1080. doi:10.2514/2.4986

[8] Inalhan, G., Tillerson, M., and How, J., "Relative Dynamics and Control of Spacecraft Formations in Eccentric Orbits," *Journal of Guidance, Control, and Dynamics*, Vol. 25, No. 1, 2002, pp. 48–59. doi:10.2514/2.4874

[9] Schaub, H., "Relative Orbit Geometry Through Classical Orbit Element Differences," *Journal of Guidance, Control, and Dynamics*, Vol. 27, No. 5, 2004, pp. 839–848. doi:10.2514/1.12595

[10] Broucke, R. A., "Solution of the Elliptic Rendezvous Problem with the Time as Independent Variable," *Journal of Guidance, Control, and Dynamics*, Vol. 26, No. 4, 2003, pp. 615–621. doi:10.2514/2.5089

[11] Zanon, D. J., and Campbell, M. E., "Optimal Planner for Spacecraft Formations in Elliptical Orbits," *Journal of Guidance, Control, and Dynamics*, Vol. 29, No. 1, 2006, pp. 161–171. doi:10.2514/1.7236

[12] Breger, L., Inalhan, G., Tillerson, M., and How, J., "Cooperative Spacecraft Formation Flying: Model Predictive Control with Open- and Closed-Loop Robustness," *Modern Astrodynamics*, edited by P. Gurfil, Elsevier Astrodynamics Series, Elsevier Ltd., Oxford, U.K., 2006, pp. 237–277, Chap. 8.

[13] Carter, T. E., and Humi, M., "Fuel-Optimal Rendezvous near a Point in General Keplerian Orbit," *Journal of Guidance, Control, and Dynamics*, Vol. 10, No. 6, 1987, pp. 567–573. doi:10.2514/3.20257

[14] Lawden, D., *Optimal Trajectories for Space Navigation*, Butterworths, London, U.K., 1963, pp. 79–86.

[15] Carter, T. E., "New Form for the Optimal Rendezvous Equations near a Keplerian Orbit," *Journal of Guidance, Control, and Dynamics*, Vol. 13, No. 1, 1990, pp. 183–186. doi:10.2514/3.20533

[16] Marec, J. P., *Optimal Space Trajectories*, Elsevier, New York, 1979, pp. 130–154.
[17] Lane, C., and Axelrad, P., "Formation Design in Eccentric Orbits Using Linearized Equations of Relative Motion," *Journal of Guidance, Control, and Dynamics*, Vol. 29, No. 1, 2006, pp. 146–160. doi:10.2514/1.13173
[18] Melton, R. G., "Time-Explicit Representation of Relative Motion Between Elliptical Orbits," *Journal of Guidance, Control, and Dynamics*, Vol. 23, No. 4, 2000, pp. 604–610. doi:10.2514/2.4605
[19] Guffanti, T., D'Amico, S., and Lavagna, M., "Long-Term Analytical Propagation of Satellite Relative Motion in Perturbed Orbits," *27th AAS/AIAA Space Flight Mechanics Meeting*, AAS Paper 17-355, Springfield, VA, 2017.
[20] Mahajan, B., Vadali, S. R., and Alfriend, K. T., "Exact Delaunay Normalization of the Perturbed Keplerian Hamiltonian with Tesseral Harmonics," *Celestial Mechanics and Dynamical Astronomy*, Vol. 130, No. 25, 2018. doi:10.1007/s10569-018-9818-8
[21] Mahajan, B., Vadali, S. R., and Alfriend, K. T., "Analytical Solution for Satellite Relative Motion: The Complete Zonal Gravitational Problem," *26th AAS/AIAA Space Flight Mechanics Meeting*, AAS Paper 16-262, Springfield, VA, 2016.
[22] Gurfil, P., and Kholshevnikov, K. V., "Distances on the Relative Spacecraft Motion Manifold," *AIAA Guidance, Navigation and Control Conference and Exhibit*, AIAA Paper 2005-5859, 2005.
[23] Gurfil, P., and Kholshevnikov, K. V., "Manifolds and Metrics in the Relative Spacecraft Motion Problem," *Journal of Guidance, Control, and Dynamics*, Vol. 29, No. 4, 2006, pp. 1004–1010. doi:10.2514/1.15531
[24] Hill, G. W., "Researches in the Lunar Theory," *American Journal of Mathematics*, Vol. 1, No. 1, 1878, pp. 5–26. doi:10.2307/2369430
[25] Gurfil, P., and Kasdin, N. J., "Nonlinear Modeling of Spacecraft Relative Motion in the Configuration Space," *Journal of Guidance, Control, and Dynamics*, Vol. 27, No. 1, 2004, pp. 154–157. doi:10.2514/1.9343
[26] Schaub, H., "Incorporating Secular Drifts into the Orbit Element Difference Description of Relative Orbits," *Advances in the Astronautical Sciences*, Vol. 114, 2003, pp. 239–258.
[27] Vallado, D. A., *Fundamentals of Astrodynamics and Applications*, 2nd ed., Microcosm Press, El Segundo, CA, 2001, pp. 604–612.
[28] Brouwer, D., "Solution of the Problem of Artificial Satellite Theory Without Drag," *The Astronomical Journal*, Vol. 64, No. 1274, 1959, pp. 378–396. doi:10.1086/107958
[29] Llorente, J. S., Agenjo, A., Carrascosa, C., de Negueruela, C., Mestreau-Garreau, A., Cropp, A., and Santovincenzo, A., "PROBA-3: Precise Formation Flying Demonstration Mission," *Acta Astronautica*, Vol. 82, No. 1, 2013, pp. 38–46. doi:10.1016/j.actaastro.2012.05.029